

# Synthesis and Characterization of $[\text{Cp}^{3i}\text{M}(\text{CO})_3]_2$ ( $\text{M} = \text{Mo}, \text{W}$ ; $\text{Cp}^{3i} = 1,2,4\text{-Triisopropylcyclopentadienyl Ligand}$ ). X-ray Crystal Structure of $[\text{Cp}^{3i}\text{Mo}(\text{CO})_3]_2$

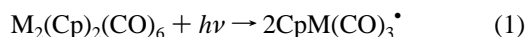
Pamela S. Tanner, Denis C. Barbini, and Wayne E. Jones, Jr.\*

Department of Chemistry, Binghamton University (SUNY), Binghamton, New York 13902-6016

Received May 9, 1997

## Introduction

The photochemistry of metal–metal-bonded dimers of the form  $\text{M}_2(\text{CO})_6(\text{C}_5\text{H}_5)_2$  has been studied extensively due to the enhanced reactivity of the odd-electron species generated upon photolysis.<sup>1–4</sup> In particular, visible excitation generates odd-electron intermediates of the form  $\text{CpM}(\text{CO})_3^*$  according to eq 1.<sup>5</sup> In order to gain a more complete picture of the electro-



chemistry of the intermediates generated upon photolysis of these dimers, we have been investigating the transient electrochemistry of complexes of the type  $\text{M}_2(\text{CO})_6(\text{R}_n\text{C}_5\text{H}_{5-n})_2$  (where  $\text{M} = \text{W}, \text{Mo}, \text{Cr}$  and  $\text{R} = \text{H}$ , halide,  $\text{CH}_3$ ).<sup>1</sup> We seek to establish a systematic correlation between ligand substitution and the observed electron transfer behavior. There is a need in this area to create a more diverse array of substituted Cp structures with significant variations in electrochemical potential following photolysis. We report here the synthesis and applicable characterization of  $[\text{Cp}^{3i}\text{M}(\text{CO})_3]_2$ , where  $\text{M} = \text{Mo}, \text{W}$  and  $\text{Cp}^{3i} = 1,2,4\text{-triisopropylcyclopentadienyl}$  ligand.

A modification of the preparation reported by Venier and Casserly readily produces triisopropyl- and tetraisopropyl-substituted cyclopentadienyl ligands<sup>6,7</sup> that can be metalated with potassium hydride.  $[\text{Cp}^{3i}\text{M}(\text{CO})_3]_2$  is readily obtained from the metal hexacarbonyl and potassium triisopropylcyclopentadienide starting materials. The use of bulky substituents on cyclopentadienyl ligands modifies the metal environment and alters the photochemistry and electrochemistry of this system relative to the unsubstituted or mono- or pentasubstituted cyclopentadienyl complexes. In addition to the modifications in the photochemistry and electrochemistry, the X-ray crystal structure analysis demonstrates several unique features in comparison to analogous dimeric complexes. These structural features may be significant for the design of future systems that involve bulky substituents.

## Experimental Section

All manipulations of air-sensitive materials were performed using standard drybox or Schlenk techniques. Elemental analyses were performed by Oneida Research Services, Inc., Whitesboro, NY. Proton NMR spectra were obtained at 360 MHz with a Bruker AM-360 spectrophotometer and referenced to the residual protons of  $\text{C}_6\text{D}_6$  ( $\delta$

7.15) or THF- $d_8$  ( $\delta$  3.58). Carbon ( $^{13}\text{C}$ ) NMR spectra were obtained at 90.5 MHz with a Bruker AM-360 spectrophotometer and referenced to the residual  $^{13}\text{C}$  resonances of  $\text{C}_6\text{D}_6$  ( $\delta$  128.0). Infrared data were obtained on a Nicolet Model 20SXC Fourier transform infrared (FTIR) spectrometer with a 1.00 mm path length NaCl solution cell ( $\text{CHCl}_3$ ). UV–vis spectra were recorded on a Hewlett-Packard 8452A diode array spectrophotometer.

**Materials.** Molybdenum hexacarbonyl and tungsten hexacarbonyl (Strem Chemicals or Aldrich) were opened and handled under nitrogen.  $\text{KCp}^{3i}$  ( $\text{Cp}^{3i} = 1,2,4\text{-}(\text{C}_3\text{H}_7)_3\text{C}_5\text{H}_2$ ) was prepared at one-third scale, as described by Williams.<sup>7,8</sup> Solvents were dried and degassed by standard methods<sup>9</sup> or purchased as SureSeal<sup>TM</sup> reagents from Aldrich. All other commercially available reagents were used without further purification.

**Synthesis of  $[\text{Cp}^{3i}\text{Mo}(\text{CO})_3]_2$ .** A modification of the preparation reported by Manning<sup>10</sup> was used to synthesize  $[\text{Cp}^{3i}\text{Mo}(\text{CO})_3]_2$ . The apparatus, consisting of a three-neck, 250 mL round-bottom flask equipped with a magnetic stirring bar, reflux condenser with gas inlet, and two stoppers, was charged with  $\text{KCp}^{3i}$  (1.40 g, 6.05 mmol) in a nitrogen drybox. The apparatus was connected to a nitrogen manifold, and a septum replaced one of the stoppers. Diglyme (50 mL) and  $\text{Mo}(\text{CO})_6$  (1.711 g, 6.48 mmol) were added to produce a deep yellow solution that was allowed to reflux for 45 min, resulting in a yellow-orange solution. Upon cooling to room temperature, methanol (1.25 mL), water (1.25 mL), and a filtered solution of  $\text{Fe}_2(\text{SO}_4)_3 \cdot 4\text{H}_2\text{O}$  (4.2 g), distilled water (66 mL), and glacial acetic acid (3.75 mL) were added using a nitrogen-purged syringe.<sup>10</sup> The resulting red solution was cooled in an ice bath. Following filtration with a Buchner funnel and washing with water, cold methanol, and hexanes, a red solid (1.042 g, 46.1%) was isolated. Purification was accomplished by recrystallization from hot acetone, resulting in an orange-red air-stable solid (0.317 g, 14%). Dec pt: 117–121 °C. Anal. Calcd for  $\text{C}_{34}\text{H}_{46}\text{Mo}_2\text{O}_6$ : C, 54.99; H, 6.24. Found: C, 54.96; H, 6.23.  $^1\text{H}$  NMR ( $\text{C}_6\text{D}_6$ ):  $\delta$  5.20 (s, 4H, ring  $-\text{CH}$ ), 2.69–2.54 (two overlapping septets, 6H,  $-\text{CHMe}_2$ ), 1.25 (d, 12H,  $-\text{CH}_3$ ), 1.13 (d, 12H,  $-\text{CH}_3$ ), 0.96 (d, 12H,  $-\text{CH}_3$ ). IR  $\nu(\text{CO})$  ( $\text{CHCl}_3$ ,  $\text{cm}^{-1}$ ): 1938 s; 1905 s; 1882 sh. UV–vis (hexanes):  $\lambda_{\text{max}}$  (nm) ( $\epsilon$ ) 408 (15 600), 494 (4530).

**Synthesis of  $[\text{Cp}^{3i}\text{W}(\text{CO})_3]_2$ .** As described above, the apparatus was charged with  $\text{KCp}^{3i}$  (1.40 g, 6.08 mmol) and anhydrous diglyme (60 mL) in a nitrogen drybox. This resulted in a brownish yellow solution. The apparatus was connected to a nitrogen manifold, and a septum replaced one of the stoppers.  $\text{W}(\text{CO})_6$  (2.198 g, 6.24 mmol) was added to produce an orange solution that was refluxed for 1 h. Upon cooling to room temperature, methanol (1.25 mL), water (1.25 mL), and a filtered solution of  $\text{Fe}_2(\text{SO}_4)_3 \cdot 5\text{H}_2\text{O}$  (4.36 g), distilled water (62.5 mL), and glacial acetic acid (3.75 mL) were added using a nitrogen-purged syringe as per Manning.<sup>10</sup> The resulting red solution was cooled in an ice bath. Following filtration with a Buchner funnel and washing with water, a red solid (1.774 g, 63.5%) was isolated. Purification was accomplished by recrystallization from hot acetone resulting in an orange-red air-stable solid (0.652 g, 23%). Dec pt: 153–163 °C. Anal. Calcd for  $\text{C}_{34}\text{H}_{46}\text{W}_2\text{O}_6$ : C, 44.46; H, 5.05. Found: C, 44.14; H, 5.03.  $^1\text{H}$  NMR ( $\text{C}_6\text{D}_6$ ):  $\delta$  5.30 (s, 4H, ring  $-\text{CH}$ ), 2.83 (septet, 2H,  $-\text{CHMe}_2$ ), 2.56 (septet, 4H,  $-\text{CHMe}_2$ ), 1.23 (d, 24H in sum with doublet at 1.17,  $-\text{CH}_3$ ), 1.17 (d,  $-\text{CH}_3$ ), 0.95 (d, 12H,  $-\text{CH}_3$ ). IR  $\nu(\text{CO})$  ( $\text{CHCl}_3$ ,  $\text{cm}^{-1}$ ): 1936 s; 1899 s; 1873 sh. UV–vis (hexanes):  $\lambda_{\text{max}}$  (nm) ( $\epsilon$ ) 376 (9350), 474 (3270).

**Electrochemistry.** An EG&G PAR 273A potentiostat coupled to a personal computer was used for all conventional electrochemical measurements. Typical ground-state electrochemical experiments were performed on  $\text{N}_2$  deoxygenated, 1.0 mM solutions of dimer in 0.1–0.2 M (TBAH)/( $\text{CH}_3\text{CN}$ , DMF). A platinum-button working electrode (8 mm BAS), a platinum-wire counter electrode, and a freshly prepared silver/silver chloride reference electrode comprised the three-electrode system used in all electrochemical experiments. All electrochemical

- (1) Barbini, D. C.; Tanner, P. S.; Francone, T. D.; Furst, K. B.; Jones, W. E., Jr. *Inorg. Chem.* **1996**, *35*, 4017.
- (2) Baker, M. L.; Bloyce, P. E.; Campen, A. K.; Rest, A. J.; Bitterwolf, T. E. *J. Chem. Soc., Dalton Trans.* **1990**, 2825.
- (3) Geoffroy, G. L. *J. Chem. Educ.* **1983**, *60*, 861.
- (4) Peters, J.; George, M. W.; Turner, J. J. *Organometallics* **1995**, *14*, 1503.
- (5) Meyer, T. J.; Caspar, J. V. *Chem. Rev.* **1985**, *85*, 187.
- (6) Venier, C. G.; Casserly, E. W. *J. Am. Chem. Soc.* **1990**, *112*, 2808.
- (7) Williams, R. A.; Tesh, K. F.; Hanusa, T. P. *J. Am. Chem. Soc.* **1991**, *113*, 4843.

- (8) Sitzmann, H.; Zhou, P.; Wolmerhauser, G. *Chem. Ber.* **1994**, *127*, 3.
- (9) Perrin, D. D.; Armarego, W. L. F. *Purification of Laboratory Chemicals*, 3rd ed.; Pergamon: Oxford, U.K., 1988.
- (10) Manning, A. R.; Hackett, P.; Birdwhistell, R.; Soye, P. *Inorg. Synth.* **1990**, *28*, 148.

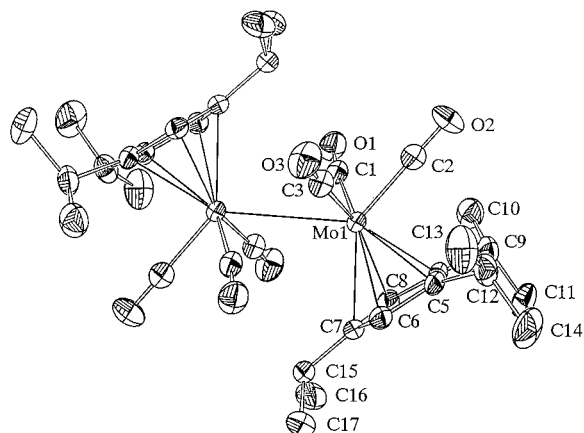


**Figure 1.** ORTEP view of  $[\text{Mo}(\text{CO})_3\{i\text{-Pr}_3\text{Cp}\}]_2$  with numbering scheme adopted. Ellipsoids are drawn at the 50% probability level. Hydrogens are omitted.

half-wave potentials were referenced to the ferrocene standard couple versus SCE. Scan rates for cyclic voltammetry ranged from 50 to 500 mV/s.

**Photomodulated Voltammetry.** The experimental setup for photomodulated voltammetry has been previously reported.<sup>1</sup> The PMV excitation was tuned to 488 nm with incident power of ~300 mW at the cell (Ophir 30A-P power meter) at modulation frequencies of 10 Hz to 1.0 kHz. The observed potentials were independent of the excitation frequency over the range of frequencies.<sup>11,12</sup> The solution of analyte (100–150 mL, 0.001 M) and supporting electrolyte (0.1–0.2 M) was deoxygenated with  $\text{N}_2$  for 15 min prior to each experiment. All electrochemical potentials were referenced to SCE using an internal ferrocene reference.

**Laser Flash Photolysis.** Transient absorption was performed at the Center for Photoinduced Charge Transfer at the University of Rochester on a system described elsewhere.<sup>13</sup> The solutions, typically 0.20 mM, were irradiated at 480 nm by an excimer pumped dye laser with a coumarin dye. Changes in absorption following excitation reversibly returned to the base line in all experiments.

**Structure Determination.** Suitable crystals for X-ray crystallographic examination of  $[\text{Cp}^{3i}\text{Mo}(\text{CO})_3]_2$  were recrystallized from hexanes. Determination of cell constants and data collection were carried out at 214(2) K on a Nonius CAD-4 diffractometer with  $\omega/2\theta$  collection. The structure was determined and refined at the University of Montreal by Dr. Andre L. Beauchamp. Additional information is available as Supporting Information.

## Results and Discussion

Potassium triisopropylcyclopentadienide was prepared at one-third scale using a versatile, one-pot technique according to the literature procedure.<sup>7,14</sup> Potassium triisopropylcyclopentadienide was allowed to react in an equimolar ratio with metal hexacarbonyls to synthesize  $[\text{Cp}^{3i}\text{M}(\text{CO})_3]_2$  dimeric complexes where  $\text{M} = \text{Mo}, \text{W}$  in a modification of the procedure reported by Manning.<sup>10</sup> The percent yields of the crude products were moderate, 46% for Mo and 63% for W. The air-stable solids were isolated and fully characterized. In addition,  $[\text{Cp}^{3i}\text{Mo}(\text{CO})_3]_2$  was characterized by single-crystal X-ray diffraction. The X-ray-determined structure, as shown in Figure 1, was supported by NMR and IR spectroscopic characterization.

The carbonyl stretching vibrations of the triisopropylcyclopentadienyl complexes were consistent with those for analogous

**Table 1.** Selected Crystal Data and Structure Refinement for  $[\text{Mo}(\text{CO})_3\{i\text{-Pr}_3\text{Cp}\}]_2$

formula	$\text{C}_{34}\text{H}_{46}\text{Mo}_2\text{O}_6$
fw	742.59
color	red
size (mm)	$0.36 \times 0.27 \times 0.07$
space group	$P\bar{1}$
$a$ (Å)	10.521(5)
$b$ (Å)	12.717(5)
$c$ (Å)	13.583(6)
$\alpha$ (deg)	103.36(3)
$\beta$ (deg)	101.20(3)
$\gamma$ (deg)	93.2 (3)
$V$ (Å <sup>3</sup> )	1724.5(13)
$Z$	2
density, $D_{\text{exptl}}$ (Mg/m <sup>3</sup> )	1.430
radiation	Cu K $\alpha$
wavelength, $\lambda$ (Å)	1.540 56
$\theta$ range (deg)	20.00–22.50
linear abs coeff, $\mu$ (mm <sup>-1</sup> )	6.39
temp (K)	214(2)
final $R$ indices, $I > 2\sigma(I)^a$	$R1 = 0.0333$ , $wR2 = 0.0890$
$R$ indices, all data <sup>a</sup>	$R1 = 0.0421$ , $wR2 = 0.0936$

$$^a R1 = \sum(|F_o| - |F_c|)/\sum|F_o|; wR2 = [\sum[w(F_o^2 - F_c^2)^2]/\sum[w(F_o^2)^2]]^{1/2}; S = [\sum[w(F_o^2 - F_c^2)^2]/(\text{no. of reflections}) - (\text{no. of params})]^{1/2}$$

complexes containing only terminal carbonyl ligands. Molecules that approach a  $C_{2h}$  symmetry display three bands in the carbonyl region.<sup>15</sup> The electronic absorption spectra<sup>16</sup> of the complexes are also consistent with the metal–metal-bonded dimeric structure. The intense near-UV band at high energy, 408 nm where  $\text{M} = \text{Mo}$  and 376 nm where  $\text{M} = \text{W}$ , is attributed to a  $\sigma \rightarrow \sigma^*$  transition.<sup>5</sup>

**Structure Determination.** The structure of the  $[\text{Cp}^{3i}\text{Mo}(\text{CO})_3]_2$  dimeric complex is generally consistent with those of analogous  $[(R_n\text{C}_5\text{H}_{5-n})\text{M}(\text{CO})_3]_2$  complexes (Table 1). The metal to metal bond distances are consistent with a Mo–Mo single bond,<sup>17</sup> and the cyclopentadienyl ligands are oriented in a centrosymmetric anti-rotational configuration.<sup>18</sup> There are, however, unusual structural features that are clearly the result of a complex balance of several factors, including the steric and electronic properties of the triisopropylcyclopentadienyl ligand. The first difference is in the presence of four  $\text{Mo}(\text{CO})_3\text{Cp}^{3i}$  units per unit cell, as shown in Figure 2. The two dimer molecules are nearly identical, with Mo–Mo bond distances of 3.220(1) and 3.224(1) Å, respectively. Refinement demonstrated that the unit cell contained two symmetry-independent molecules,  $\text{Mo}(1)\text{--}\text{Mo}(1)^a$  and  $\text{Mo}(2)\text{--}\text{Mo}(2)^a$ , both perfectly centrosymmetric. This type of situation has been observed previously for triclinic crystals with two independent molecules per asymmetric unit.<sup>19</sup> We have been unable to find any previous examples of dimeric complexes that demonstrate this two-molecule structure.

Another unusual structural feature is the apparent shortening of the Mo–Mo bond (Table 2). On the basis of electron-donating considerations one would expect the metal–metal bond in  $[\text{Cp}^{3i}\text{Mo}(\text{CO})_3]_2$  to be longer than that of  $[\text{Cp}^*\text{Mo}(\text{CO})_3]_2$ , shorter than that of  $[\text{Cp}^{\text{B}}\text{Mo}(\text{CO})_3]_2$ , and similar to that of  $[\text{Cp}^{2i\text{-Bu}}\text{Mo}(\text{CO})_3]_2$ . This is clearly not the case. The  $[\text{Cp}^{3i}\text{Mo}(\text{CO})_3]_2$  dimers have Mo–Mo bond distances of 3.220(1)

(11) Nagaoka, T.; Griller, D.; Wayner, D. D. M. *J. Phys. Chem.* **1991**, *95*, 6264.

(12) Wayner, D. D. M.; McPhee, D. J.; Griller, D. *J. Am. Chem. Soc.* **1988**, *110*, 132.

(13) Chen, L.; Farahat, M. S.; Gaillard, E. R.; Farid, S.; Whitten, D. G. *Photochem. Photobiol. A: Chem.* **1996**, *95*, 21.

(14) Burman, J. A.; Hays, M. L.; Burkey, D. J.; Tanner, P. S.; Hanusa, T. P. *J. Organomet. Chem.* **1994**, *479*, 135.

(15) Parker, D. J. *J. Chem. Soc., Dalton Trans.* **1974**, 155.

(16) Fei, M.; Sur, S. K.; Tyler, D. R. *Organometallics* **1991**, *10*, 419.

(17) Curtis, M. D.; Williams, P. D.; Butler, W. M. *Inorg. Chem.* **1988**, *27*, 2853.

(18) Adams, R. D.; Collins, D. E.; Cotton, F. A. *J. Am. Chem. Soc.* **1974**, *96*, 749.

(19) (a) Lebuis, A. M.; Beauchamp, A. L. *Can. J. Chem.* **1993**, *71*, 441.

(b) Johnson, J. W.; Brody, J. F.; Ansell, G. B.; Zentz, S. *Inorg. Chem.* **1984**, *23*, 2415.

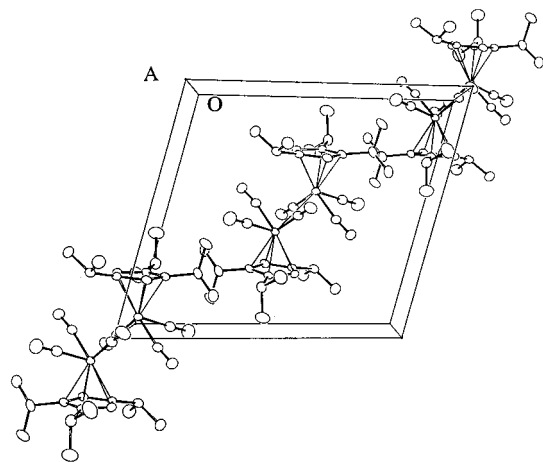


**Figure 2.** Unit cell of  $[\text{Mo}(\text{CO})_3\{i\text{-Pr}_3\text{Cp}\}]_2$  containing four monomer units.

**Table 2.** Selected Bond Lengths (Å) and Angles (deg) for  $[\text{Mo}(\text{CO})_3\{i\text{-Pr}_3\text{Cp}\}]_2$

Mo(1)–Mo(1) <sup>a</sup>	3.220(1)	C(4)–C(5)	1.444(4)
Mo(1)–C(1)	1.973(3)	C(4)–C(9)	1.516(4)
Mo(1)–C(2)	1.953(3)	C(5)–C(6)	1.419(4)
Mo(1)–C(3)	1.992(3)	C(5)–C(12)	1.510(4)
Mo(1)–C(4)	2.318(3)	C(6)–C(7)	1.422(4)
Mo(1)–C(5)	2.313(3)	C(7)–C(8)	1.427(4)
Mo(1)–C(6)	2.363(3)	C(7)–C(15)	1.516(4)
Mo(1)–C(7)	2.444(3)	C(1)–O(1)	1.153(4)
Mo(1)–C(8)	2.356(3)	C(2)–O(2)	1.151(4)
C(4)–C(8)	1.425(4)	C(3)–O(3)	1.148(4)
C(1)–Mo(1)–C(2)	79.05(14)	C(2)–Mo(1)–Mo(1) <sup>a</sup>	126.46(9)
C(1)–Mo(1)–C(3)	106.90(13)	C(1)–Mo(1)–Mo(1) <sup>a</sup>	68.99(9)
C(2)–Mo(1)–C(3)	79.35(13)	C(3)–Mo(1)–Mo(1) <sup>a</sup>	70.87(9)
C(2)–Mo(1)–C(5)	85.14(12)	C(5)–Mo(1)–Mo(1) <sup>a</sup>	144.72(7)
C(1)–Mo(1)–C(5)	140.60(11)	C(4)–Mo(1)–Mo(1) <sup>a</sup>	143.96(7)
C(3)–Mo(1)–C(5)	105.23(12)	C(8)–Mo(1)–Mo(1) <sup>a</sup>	108.50(7)
C(2)–Mo(1)–C(4)	84.89(11)	C(6)–Mo(1)–Mo(1) <sup>a</sup>	109.42(7)
C(1)–Mo(1)–C(4)	105.86(11)	C(7)–Mo(1)–Mo(1) <sup>a</sup>	92.30(7)
C(3)–Mo(1)–C(4)	139.93(12)	C(8)–C(4)–Mo(1)	73.74(14)
C(5)–Mo(1)–C(4)	36.34(10)	C(5)–C(4)–Mo(1)	71.7(2)
C(2)–Mo(1)–C(8)	117.19(11)	C(9)–C(4)–Mo(1)	127.3(2)
C(1)–Mo(1)–C(8)	96.78(12)	C(6)–C(5)–Mo(1)	74.3(2)
C(3)–Mo(1)–C(8)	153.66(12)	C(5)–C(4)–Mo(1)	72.0(2)
C(5)–Mo(1)–C(8)	59.29(10)	C(12)–C(5)–Mo(1)	127.8(2)
C(4)–Mo(1)–C(8)	35.50(9)	C(5)–C(6)–Mo(1)	70.4(2)
C(5)–Mo(1)–C(6)	35.31(9)	C(7)–C(6)–Mo(1)	75.9(2)
C(4)–Mo(1)–C(6)	58.98(10)	C(6)–C(7)–Mo(1)	69.7(2)
C(8)–Mo(1)–C(6)	57.95(10)	C(8)–C(7)–Mo(1)	69.39(14)
C(5)–Mo(1)–C(7)	58.35(9)	C(15)–C(7)–Mo(1)	133.0(2)
C(4)–Mo(1)–C(7)	58.35(9)	C(4)–C(8)–Mo(1)	70.77(14)
C(8)–Mo(1)–C(7)	34.53(10)	C(7)–C(8)–Mo(1)	76.1(2)
C(6)–Mo(1)–C(7)	34.36(9)		

and 3.224(1) Å, respectively. In comparison to other analogues,  $[\text{CpMo}(\text{CO})_3]_2$  (3.235(1) Å),<sup>20</sup>  $[\text{Cp}^{2t\text{-Bu}}\text{Mo}(\text{CO})_3]_2$  (3.253(1) Å),<sup>21</sup> and  $[\text{Cp}^*\text{Mo}(\text{CO})_3]_2$  (3.281(1) Å),<sup>22</sup> the dimer exhibits a metal–metal bond length that is much shorter than expected.

**Dimer Electrochemistry.** Electrochemical characterization was performed on  $[\text{Cp}^*\text{Mo}(\text{CO})_3]_2$  and  $[\text{Cp}^*\text{W}(\text{CO})_3]_2$  in DMF and  $\text{CH}_3\text{CN}$ . Cyclic voltammetry shows four irreversible couples in both DMF and  $\text{CH}_3\text{CN}$ , consistent with previous results on Mo and W dimers of this type.<sup>1–3,23</sup> Shown in Table

**Table 3.** Room-Temperature Cyclic Voltammetry of Dimeric Complexes<sup>a</sup>

compd	solvent	I <sup>b</sup>	II <sup>c</sup>	III <sup>d</sup>	IV <sup>e</sup>
$(\eta^5\text{-C}_5\text{H}_5)_2\text{W}_2(\text{CO})_6$	$\text{CH}_3\text{CN}$	–1.28	–0.06	1.03	–0.67
	DMF	–1.34	–0.05	1.07	–0.61
$(\eta^5\text{-Cp}^{3i})_2\text{W}_2(\text{CO})_6$	$\text{CH}_3\text{CN}$	–1.39	–0.16	0.92	–0.76
	DMF	–1.48	–0.13	0.94	–0.72
$(\eta^5\text{-C}_5\text{H}_5)_2\text{Mo}_2(\text{CO})_6$	$\text{CH}_3\text{CN}$	–1.13	–0.09	1.00	–0.60
	DMF	–1.05	–0.02	1.10	–0.39
$(\eta^5\text{-Cp}^{3i})_2\text{Mo}_2(\text{CO})_6$	$\text{CH}_3\text{CN}$	–1.44	–0.18	0.95	–0.77
	DMF	–1.50	–0.14	0.97	–0.73

<sup>a</sup> Reported as peak potentials ( $\pm 0.03$  V) vs SCE at a scan rate of 250 mV/s. All solutions were 1 mM analyte in 0.2 M TBAH/solvent and were bubble-deoxygenated for 10 min using  $\text{N}_2$ . <sup>b</sup> Reaction I corresponds to dimer reduction:  $2e^- + \text{M}_2(\text{Cp})_2(\text{CO})_6 \rightarrow 2\text{M}(\text{Cp})(\text{CO})_3^-$ . <sup>c</sup> Reaction II corresponds to anion oxidation:  $2\text{M}(\text{Cp})(\text{CO})_3^- \rightarrow \text{M}_2(\text{Cp})_2(\text{CO})_6 + 2e^-$ . <sup>d</sup> Reaction III corresponds to dimer oxidation:  $\text{M}_2(\text{Cp})_2(\text{CO})_6 \rightarrow 2\text{M}(\text{Cp})(\text{CO})_3^+ + 2e^-$ . <sup>e</sup> Reaction IV corresponds to cation reduction:  $2\text{M}(\text{Cp})(\text{CO})_3^+(\text{solvent})^+ + 2e^- \rightarrow \text{M}_2(\text{Cp})_2(\text{CO})_6$ .

3 are the peak potentials for each of the four irreversible waves along with analogous data for related systems. A negative shift in potential is observed in going from Cp- to Cp<sup>3i</sup>-substituted complexes for all four processes, consistent with previously observed changes upon substitution of electron-donating substituents.<sup>24</sup>

However, the potential application of this system within a larger series of electrochemical potentials may be called into question. The shorter M–M bond length could suggest that there will be differences in the recombination rate of the radicals to form the dimer following photolysis. The irreversible peak potentials could therefore be substantially shifted by kinetic variations at the electrode.

**Transient Characterization.** In order to more accurately place these new systems within the larger series of dimers that are being investigated, transient electrochemical and spectroscopic techniques were utilized.<sup>1</sup> Direct electrochemical observation of the odd-electron complexes was achieved using photomodulated voltammetry (PMV), as demonstrated for analogous complexes previously.<sup>1,12</sup> PMV results in deoxygenated DMF solution show reduction potentials of  $-0.21 \pm 0.05$  and  $-0.25 \pm 0.1$  V vs SCE for  $\text{Cp}^{3i}(\text{CO})_3\text{W}^\bullet$  and  $\text{Cp}^{3i}(\text{CO})_3\text{Mo}^\bullet$ , respectively. These results, in comparison to PMV on model Cp systems,<sup>1</sup> are consistent with the increased electron-donating properties of the isopropyl-substituted cyclopentadienyl ligand, as seen previously for ferrocene derivatives.<sup>24</sup>

Time-resolved absorption spectroscopy was used to determine the kinetics of the recombination rate of the radicals to re-form the dimer complex following photolysis (Figure 3). The results from excitation into the lowest energy absorption at 480 nm for both Mo and W dimer complexes indicated a second-order recombination process for the radicals (eq 2). In each case, a



loss of absorption was observed in the 350–450 nm region of the spectrum, where the dimer complex absorbed prior to photolysis. These results correspond directly to previous flash photolysis results on  $\text{MCp}(\text{CO})_3^\bullet$  systems.<sup>5,25</sup> Second-order recombination rates of  $(5.6 \pm 0.3) \times 10^8 \text{ M}^{-1} \text{ s}^{-1}$  were observed for the tungsten complex and  $(8.3 \pm 0.4) \times 10^8 \text{ M}^{-1} \text{ s}^{-1}$  for the molybdenum complex. These data represent a decrease of nearly an order of magnitude in recombination rate relative to

(20) Adams, R. D.; Collins, D. M.; Cotton, F. A. *Inorg. Chem.* **1974**, *13*, 1086.

(21) Hughes, R. P.; Lomphey, J. R.; Rheingold, A. L.; Yap, G. P. A. *J. Organomet. Chem.* **1996**, *517*, 63.

(22) Clegg, W.; Compton, N. A.; Errington, J. A.; Norman, N. C. *Acta Crystallogr., Sect. C* **1988**, *44*, 568.

(23) Kadish, K. M.; Lacombe, D. A.; Anderson, J. E. *Inorg. Chem.* **1986**, *25*, 2246.

(24) Geiger, W. E. In *Organometallic Radical Processes*; Troglor, W. C., Ed.; Elsevier: New York, 1990; p 142.

(25) Pugh, J. R.; Meyer, T. J. *J. Am. Chem. Soc.* **1992**, *114*, 3784.

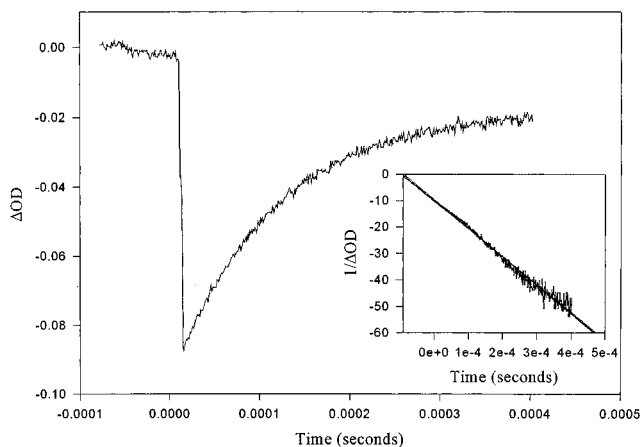


**Figure 3.** Transient absorption trace of  $(\text{Cp}^{3i}\text{W}(\text{CO})_3)_2$  in DMF with second-order fit.

the methyl-substituted Cp systems.<sup>5,25</sup> This decrease in recombination rate is best explained by the potential steric interactions that exist due to isopropyl substitution of the cyclopentadiene ligands.

On the basis of the transient characterization, IR spectroscopy, and electrochemistry, we conclude that the change in the electronic structure induced by substitution is dominated by the electron-donating ability of the isopropyl substituents. The substantial change in the recombination rate observed spectroscopically also points to significant steric interactions, since electronic effects alone do not account for the order of magnitude shift. The potential steric interactions observed in the X-ray structure were consistent with the decreased recombination rate.

The basis for the shorter metal–metal bond distance in the  $[\text{Cp}^{3i}\text{Mo}(\text{CO})_3]_2$  dimer is unclear. Steric interactions would predict that the triisopropyl-substituted Cp may have the greatest M–M bond length. Similar to earlier reports on  $[\text{Cp}^{2t\text{-Bu}}\text{Mo}(\text{CO})_3]_2$ ,<sup>25</sup> electronic interactions appear to result in a shorter bond length. The fact that the final M–M distance for  $[\text{Cp}^{3i}\text{Mo}(\text{CO})_3]_2$  is shorter than unsubstituted Cp dimers cannot be completely accounted for in this manner. There must be an additional interaction in the crystal which decreases the M–M bond length. On the basis of the IR data and the metal–carbonyl distances, a semibridging carbonyl can be ruled out. While positive interactions between the isopropyl substituents may be occurring, further work is necessary to identify the source of this additional interaction.

**Acknowledgment.** We wish to thank Prof. André Beauchamp for his assistance in collecting and resolving the X-ray structure, Prof. Timothy Hanusa for insights on the resulting  $\text{Cp}^{3i}$  complexes, Dr. Tim Rhodes and the NSF-Center for Photoinduced Charge Transfer at the University of Rochester for assistance with the laser flash photolysis experiments, and Dr. Stan Madan for helpful discussions. Financial support for this work was provided by the Petroleum Research Fund under Grant Nos. 28702-G3 and 31539-AC3 and the Research Foundation of the State University of New York.

**Supporting Information Available:** An X-ray crystallographic file, in CIF format, for the structure of  $\text{C}_{34}\text{H}_{46}\text{Mo}_2\text{O}_6$  is available on the Internet only. See any current masthead page for access information.

IC970547N